Hindawi
Advances in Materials Science and Engineering
Volume 2020, Article ID 7267808, 8 pages
https://doi.org/10.1155/2020/7267808

Research Article

Corrosion Localization Analysis in T-Shape Pipe Junction Based on Multielectrode Current Measurements

Georgii S. Vasyliev

Department of Chemical Technology, National Technical University of Ukraine "Igor Sikorsky Kyiv Polytechnic Institute", Kyiv 03056, Ukraine

Correspondence should be addressed to Georgii S. Vasyliev; g.vasyliev@kpi.ua

Received 16 August 2020; Revised 2 October 2020; Accepted 8 October 2020; Published 26 October 2020

Academic Editor: Marian Palcut

The water flow rate and galvanic current distribution in the T-shape junction of steel pipes were investigated using the multielectrode array approach. The inner surface of polypropylene pipes junction was divided into 15 separate sections, and a steel plate was placed in every section to form a single inner surface. The tap water flow rate varied between 0.28 and 0.57 m/s, and the water distribution in the junction was between 5 : 1 and 1 : 5. The galvanic current flowing through each steel electrode was mapped on the 3D model of the T-shape junction. Two differential aeration pairs were found with high anodic current densities.

1. Introduction

Water distribution networks for domestic and industrial needs, manufactured from steel pipes, are vulnerable to internal corrosion. Dissolved gases, mainly O_2 and CO_2, as well as dissolved salts cause corrosion aggressivity of the water. Internal corrosion of pipelines leads to water quality deterioration; appearance of iron, taste, and color may lead to health problems for water consumers [1]. Furthermore, corrosion shortens the operation time of pipes and leads to unpredicted failures and water supply interruptions [2–5]. The solution of corrosion problems in water networks remains a challenging task nowadays.

In addition to general corrosion, caused mainly by oxygen, water networks include large number of pipe junctions and turns. When flow passes through these elements, water velocity deviates from the mean value in different parts of the junction. Change in the flow rate leads to the different oxygen supply causing the formation of differential aeration galvanic couples between parts of the surface with dissimilar flow rate [6, 7]. The operation of anodic region of galvanic couple accelerates metal dissolution and even leads to the penetration of the pipe wall within a short period. Chang et al. investigated the formation of a differential aeration cells in the pipe when the layer of deposits was formed on the inner surface. Low oxygen supply under the covered part of the surface resulted in the formation of the anodic region, while the remaining surface acted as a cathode. In the proposed model, the formation of anodic and cathodic regions was not assumed from the beginning, but they were formed during the modeling [8]. Differential aeration cells are also formed during pipe corrosion due to soil corrosiveness. Due to the low oxygen diffusion rate in soil, the part of the pipe which is closer to the ground becomes cathodic, and the bottom part becomes anodic and dissolves faster [9, 10].

The investigation of differential aeration cells is based on the galvanic current measurement between at least two electrodes. In [11], the authors measured the galvanic current between two pairs of short-circuit electrodes placed in both sides of a confuser. The rate of seawater flow changed from 0.5 to 5 m/s when going through the confuser, and the electrode placed at the lower flow rate region became anodic. The measured current density between the electrodes reached 100 $\mu A/cm^2$.

In recent years, multielectrode techniques are used to investigate the localization of corrosion in polymetallic systems [12, 13], under coatings [14], in crevices, or under cathodic protection [15, 16]. The working electrodes or coupled multielectrode array sensors (CMASs) consist of a

pack of electrodes sealed with epoxy resin with only one side remaining open to the solution. The number of the electrodes varies from 16 to 100 but is not limited. All the electrodes are interconnected through the digital zero-resistance ammeter, allowing the measurement of the galvanic currents flowing through each electrode individually.

The application of multielectrode array allowed Naganuma et al. to investigate current distribution in the crevice [17]. The distribution of anodic and cathodic regions was consistent with oxygen supply—cathodic regions were in the top part, while anodic were in the bottom part, where oxygen supply was limited. Galvanic current was found to be lower for narrower crevices.

Multielectrode was successfully applied to study the localization of corrosion process under cathodic protection [18, 19]. The distribution of anodic regions was mapped, and a strong correlation was established between measured currents flowing through the electrodes and ex situ measurements of corrosion degradation.

An array of microelectrodes was used to investigate the formation of galvanic couples under the seawater droplet on the zinc surface. The localization of the anodic region was established in the center of the droplet, while cathodic region was located around it. The instantaneous current below 1 μA flowing through each wire was measured, the total anodic and cathodic currents were determined. The application of multielectrode array technique enabled the localization of anodic regions in the exceedingly small area of 0.25 mm^2.

A recent work reports the investigation of flow-induced corrosion and erosion corrosion with multielectrode array system [20]. The multielectrode consisted of 100 separate wires of 5.02 mm^2 square, all sealed with polymer and connected to the multiplexer. The electrode was placed in the cell, and the desirable flow rate was maintained with propeller stirrer. The application of multielectrode allowed the establishment of the surface distribution on anodic and cathodic regions as well as the current values flowing through each electrode. Maximum anodic current was found to exceed 80 μA, while the total anodic current reached 800 μA.

The literature survey shows that multielectrode technique is a promising approach to studying the localization of corrosion processes that allows in situ determining of the localization of anodic regions and local current values. However, no data is reported on the operation of galvanic cells that are formed in metal pipes due to flow inhomogeneity. In this work, the T-shape junction was chosen to investigate galvanic current distribution at different flow rates and flow distributions. This will allow us to predict the localization of anodic regions, establish local dissolution rate, and plan corrosion prevention measures.

1.1. Flow Rate Distribution and Differential Aeration Cell Operation. The T-shape junction is commonly used in water distribution networks, mainly to connect pipes in different parts of the network. This simple type of pipe connection is easily installed in the system; however, it causes serious flow distribution because of the sharp angle between the pipes. When water flow at high velocity is divided between main channel and side channel, the regions of high and low flow rate appear. To study the distribution of these zones in the T-shape junction, a computer model was built using COMSOL Multiphysics 5.2 software. The 2D-model consists of a T-shape junction of 50 and 40 mm size. The water flows with a flow rate of 0.28–0.57 m/s. Depending on the distribution ratio between main and side pipes, flow rate diagrams are presented in Figure 1.

When the flow distribution is 5 : 1, the main part of the water is passing through the main channel, the remaining water in the side channel has the same velocity value. However, the flow rate distributions in the main and side channels are different. The water flow is localized only in a thin line near the side channel upper wall. The residual part of the side channel is a stagnant zone. In the meantime, the flow rate in the main channel remains constant through the pipe. Such flow distribution is observed independently of water flow rate.

The change in water distribution to 1 : 1 causes acceleration of water flow rate in the side channel. Moreover, high water flows in this condition occupy half of the side channel cross section. The water flow rate is also changed: it is increased 1.5 times in the side channel and decreased in the main channel after the junction. The new stagnant zone is formed in the left part of the main channel after the junction.

At last, when water distribution is 1 : 5, mainly all the flow is directed through the side channel. The flow rate in the side channel is doubled, compared to the inlet flow rate. Two distinguished stagnant zones are observed: one in the bottom wall in the side channel and another one in the left part of the main channel after the junction.

The galvanic couples in the steel pipes mainly occur between two or more regions with different flow conditions. The supply of the oxygen to the metal surface is diffusion-controlled, and the oxygen reduction current can be calculated by Levich equation:

$$i = \frac{nF\,D}{\delta_d}\,c_0, \tag{1}$$

where i is the oxygen reduction current density, A/cm^2; n is the number of electrons in oxygen reduction reaction; D is the oxygen diffusion coefficient, m^2/sec; c_0 is the oxygen concentration in the bulk of electrolyte, mole/cm^3; and δ_d is the diffusion layer thickness, cm. δ_d is known to depend on the thickness of boundary layer δ_b where the water flow rate changes from bulk to surface, which is in reverse proportion to the flow rate. Therefore, the higher the flow rate, the thinner the diffusion layer and the higher the oxygen reduction current. Thus, water flow rate at a certain surface area determines oxygen supply and reduction rates.

When water flow rate in two regions is different, this may cause the formation of the aeration galvanic cell. The part of the surface with low flow rate becomes anodic, due to low oxygen supply, and another region with higher flow rate becomes cathodic, where oxygen reduction mainly occurs.

Water conductivity determines the distance between the regions. Low conductivity of water means that these

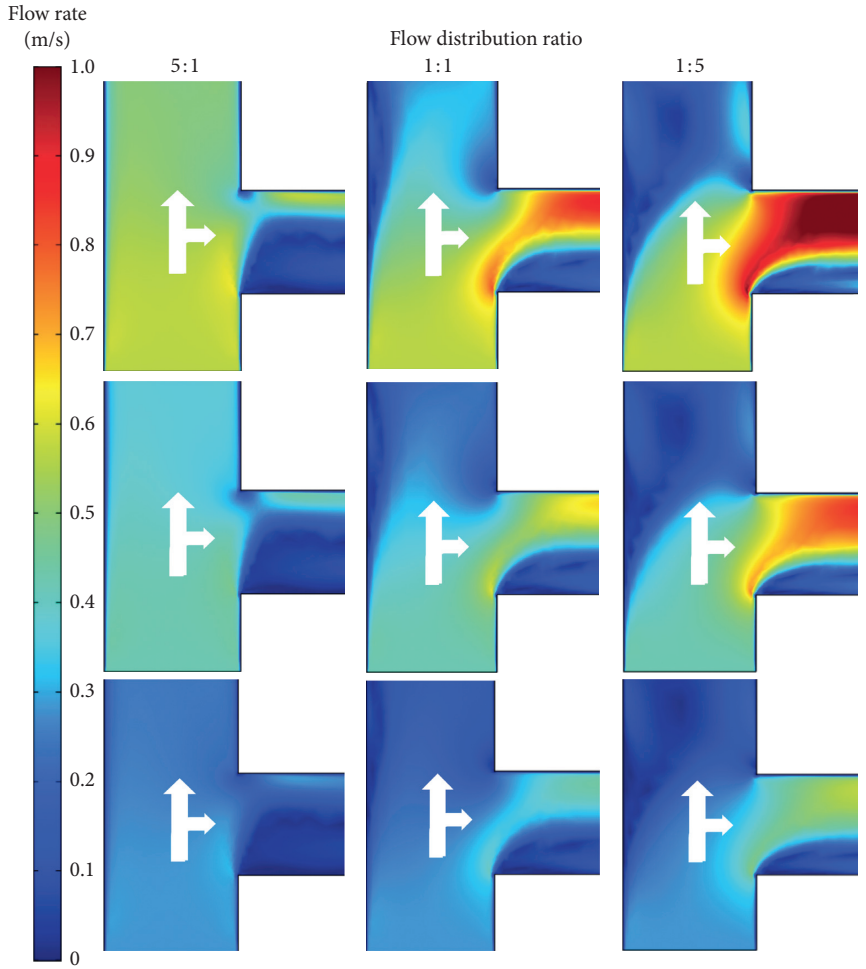

Figure 1: Flow velocity distribution in T-shape junction at various flow rates and flow distribution ratios.

regions are to be close to one another, and high conductivity allows the galvanic couple to operate in a larger distance. In addition, the higher the difference in flow rates is, the longer the distance can be between anodic and cathodic regions.

The analysis of flow distribution in T-shape junction (Figure 1) allows us to predict several possible aeration galvanic couples. The flow rate in the bottom part of the side channel is always low. This means that this part should be anodic. Another part where the flow rate decreases is the left wall of the main channel after the junction. When the flow ratio is between 1 : 1 and 1 : 5, another anodic region may occur. Cathodic regions are mainly localized near the regions where flow rate is high. They are the top part of the side channel, the right wall of the main channel before the junction. The formation of these couples can be predicted from flow rate analysis.

The rate of metal dissolution in the anodic regions can be easily recalculated in corrosion rate (CR) value. In practice, corrosion rate is presented in the rate of metal wall penetration in mm/year. To obtain this parameter from the current value, Faraday's law can be used:

$$\mathrm{CR} = \frac{M \cdot i_{\mathrm{corr}} \cdot \tau \cdot 10}{n \cdot F \cdot d}, \quad (2)$$

where CR is the corrosion rate, mm/year; M is the molecular weight of the corroded metal, g; i_{corr} is the corrosion current density, A/cm^2; τ is the duration, h (1 year = 8760 hours); 10 is the recalculation coefficient, mm/cm; n is the number of electrons in the metal ionization reaction; F is the Faraday constant, A h; and d is the metal density, g/cm^3. According to (2), the anodic current density of 1 mA/cm^2 gives the corrosion rate of 0.012 mm/year for the steel pipe.

2. Materials and Methods

To measure the galvanic current distribution in the pipe junction, a self-made module was developed. The polypropylene (PP) pipe of 50 mm diameter with a junction of 40 mm diameter was used as a base. The internal surface of the T-shape junction was divided into 15 separate regions with attached steel plate electrodes (Figure 2). On the inner side of each region, the piece of steel sheet, 20 × 40 mm, was glued using silicon resin avoiding any solution ingress under the plate.

The steel plates were cut from the line of mild steel Fe37-3FN of 0.5 mm thickness, which is commonly used for construction of water networks. The steel

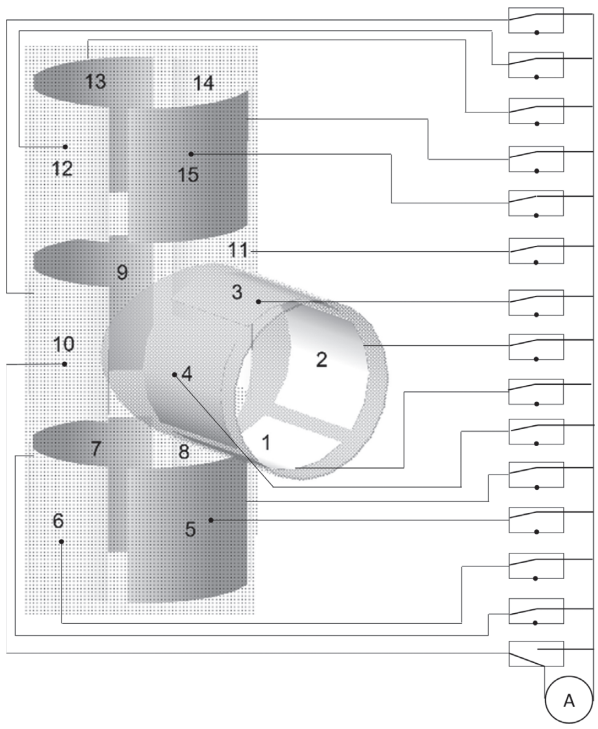

Figure 2: The multielectrode unit located inside T-shape pipe junction and electrodes wiring scheme.

composition was as follows: 0.20% C, 0.43% Mn, 0.23% Si, 0.016% S, and 0.02% P and Fe (bal.). The steel electrodes were polished mechanically with a grid paper grade P500 (R_a value of 0.1), degreased with sodium bicarbonate, and etched in 200 g/l HCl for 3–5 min. Concentrated acid was used to clean steel surface quickly and ensure the removal of any corrosion products. The wires were connected to the plates from the outer side of the pipe. All the wires were interconnected through the manual commutator that allowed us to measure galvanic currents flowing through each plate. The switch was placed in every line, allowing to us connect the ammeter to each electrode.

The T-shape junction was installed into the laboratory setup which models the operation of the circulating water system (Figure 3). Circulating loop was constructed from 50 mm PP pipes. The volume of the loop was 6 L, and Teflon fittings were used to connect PP pipes with the centrifugal pump 1, valves 4, and water heaters 2.

Prior to each test, the T-shape junction module was cleaned from any corrosion products by treatment in 200 g/l HCl solution. After cleaning, the module was washed in water flow and installed in the water circuit. The water circuit was filled with tap water of the following composition: total hardness of 200 mg/l as $CaCO_3$, total dissolved solids 240 mg/l, chlorides 20 mg/l, sulphates 30 mg/l, and dissolved oxygen 8 mg/l.

Water flow rate was regulated with the pump, and water distribution ratio in the junction was controlled using the valves 4 and flow meter 3. All the tested regimes are presented in Table 1.

The current measurements were performed manually with UNI-T UT61B multimeter (0.1 μA accuracy). Commutators allowed us to connect the ammeter to each electrode separately without disturbing the current flow in the system; the wiring scheme is given in Figure 2. The current in each line was measured continuously during 90 min. This time was found to be enough for the current to become constant. Total anodic and total cathodic currents were calculated as an algebraic sum of the separate anodic and cathodic current values passing through each electrode.

3. Results and Discussion

Typical current-time dependence is presented in Figure 4. Total anodic and total cathodic current show similar trends, and the difference between them reaches zero value, meaning the multielectrode array operates as a single system. The current dependency of separate electrodes (Figure 4(b)) shows some fluctuations with time during initial 60 min. Several electrodes keep the same current value during the whole test. The largest number of the electrodes keeps the current direction but changes the current value. Several plates change both the current direction and the value.

The period between 60 and 90 min shows no current fluctuations, meaning 60 min is enough to establish a stationary distribution of anodic and cathodic zones inside the T-shape junction. The analysis of the current-type dependencies in all conditions listed in Table 1 showed that neither the flow acceleration nor the water distribution variation changes the duration of stabilization period.

Figure 5 demonstrates the influence of flow rate and water temperature on the total anodic current. The total current depends on both the water flow rate and the flow distribution ratio between main and side channels. The rise of flow rate from 0.28 to 0.57 m/s increases the total galvanic current. The flow distribution also influences the value of the total current. The minimum current values are observed in the central part of the plot, in moderate water distribution ratios between 2.5 : 1 and 1 : 2.5. In this condition, the total current is 1.5–3 times lower compared to more extreme ratios 5 : 1 and 1 : 5. Such current dependence is explained by the fact that when the flow is distributed equally, the flow rates in the main and side channels have close values.

The number of anodic regions depending on flow rate is given in Figure 6. The water distribution ratio does not cause any changes in the number of anodic regions. However, the main influence is caused by the water flow rate. The rise of flow rate decreases the number of anodic regions, meaning the rise of galvanic current on residual anodes and further localization of corrosion process. Coupled with high total galvanic current value, the decrease in the number of anodic regions makes the T-shape junction more vulnerable to local corrosion attacks.

Local galvanic current distribution is mapped on the 3D model of T-shape pipe junction (Figure 7). The 3D model was drawn using KOMPAS-3D software. The distribution of cathodic and anodic regions depends on both the flow rate and the flow distribution. The most common anodic region, according to current measurements, is located in the bottom

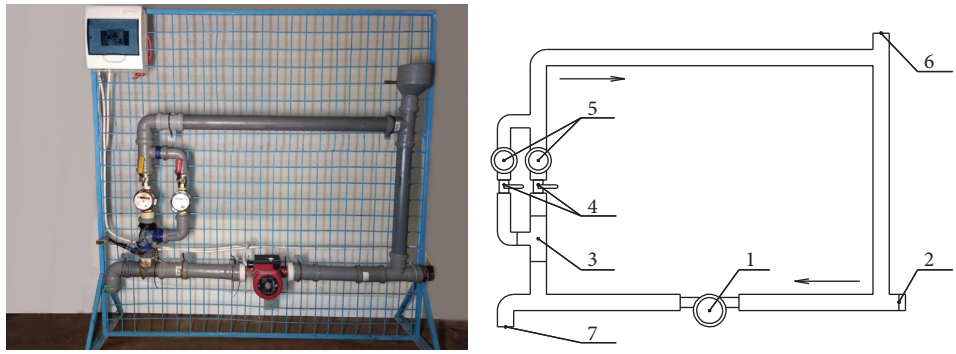

Figure 3: The photo and the scheme of laboratory setup to model the operation of water supply system: 1: centrifugal pump; 2: electric water heater; 3: multielectrode unit of the T-shape junction; 4: valves; 5: flow meters; 6: water inlet; 7: water outlet.

Table 1: Test conditions in model setup.

Temperature (°C)	Flow rate (m/s)	Flow distribution ratio Main channel : side channel				
20	0.28	5 : 1	2.5 : 1	1 : 1	1 : 2.5	1 : 5
	0.42	5 : 1	2.5 : 1	1 : 1	1 : 2.5	1 : 5
	0.57	5 : 1	2.5 : 1	1 : 1	1 : 2.5	1 : 5

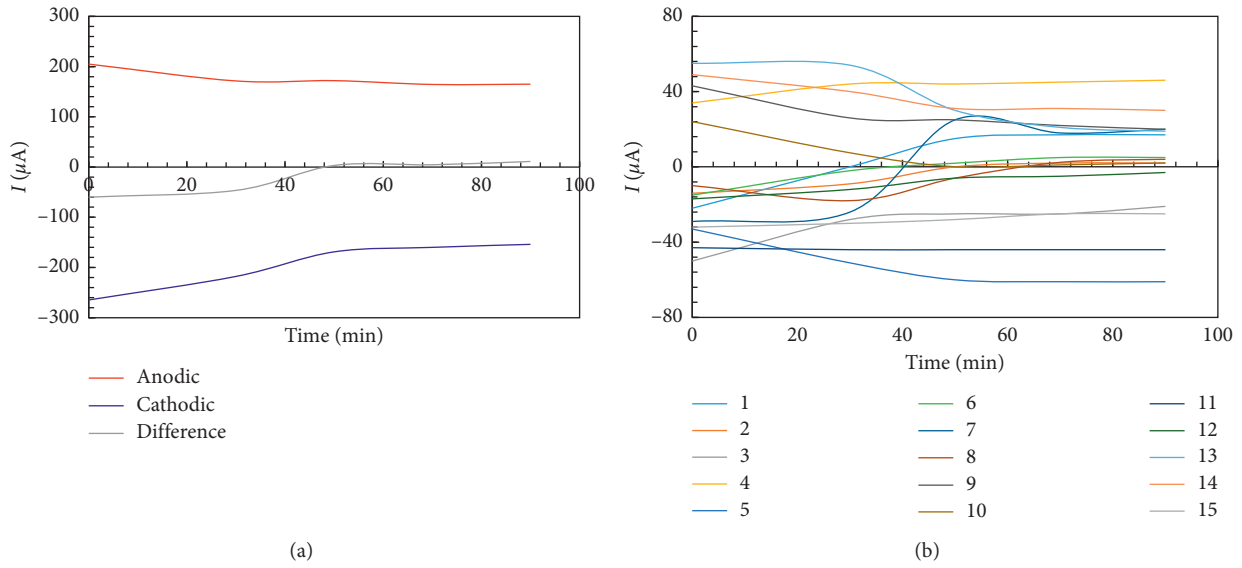

Figure 4: Typical time dependence of galvanic current in the multielectrode unit during single test: (a) total current; (b) current flowing through separate electrodes.

part of the side channel (electrode 1, Figure 2(a)). The flow divides and turns, the flow rate drops down forming a stagnant region according to the flow rate distribution map (Figure 1). The anodic current density value in this region varies in the wide range, but this electrode never shows cathodic behavior. Another anodic region is found in the left part of the main channel after the junction (electrodes 12–14, Figure 2(a)). Here, the flow rate slows because part of the water goes through the side channel.

Most commonly, cathodic regions of aeration pairs are located closely around the anodic regions due to low conductivity of potable water. The cathodic regions of electrode 1 are found to be the side walls of the side channel and the right part of the main channel before the junction electrodes 2, 4, and 5, respectively. At the same time, cathodes of the 12–14 electrodes are electrodes 9 and 15.

The anodic current density depends on the flow rate. According to the current map (Figure 7), the highest anodic current density (25 μA/cm^2 and higher) in electrode 1 is observed when water distribution is 5 : 1—water flows mainly through the main channel and independently of water distribution when flow rate is 0.57 m/s. According to (2), such a current density results in a corrosion rate of 0.3 mm/year. At lower flow rates, 0.27–0.42 m/s, and when

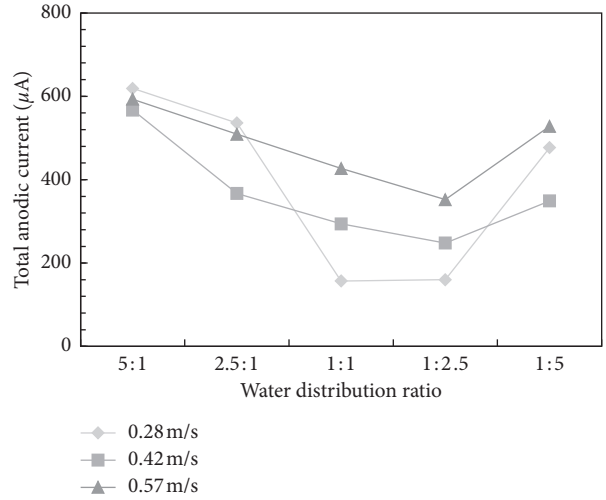

Figure 5: Total current dependence on the flow rate and flow distribution ratio.

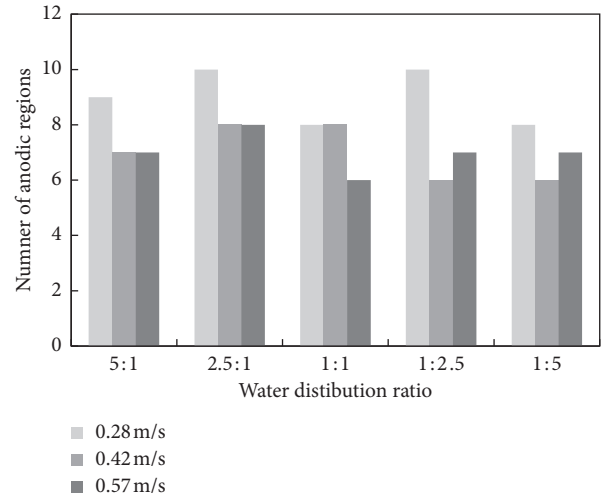

Figure 6: The number of anodic regions in T-shape junction depending on water flow rate and distribution ratio.

water distribution through the side channel is higher, the current density on electrode 1 decreases 2–5 times. The lowest anodic current density on electrode 1, below 1 μA/cm^2, was found at the lowest tested flow rate 0.28 m/s and equal water distribution through the junction (1 : 1).

The anodic region located in the part of the main channel after the junction shows (electrodes 12–14) similar behavior to electrode 1. High flow rate and water distribution 5 : 1 enable high anodic current density in this region. The highest anodic current density of 12–25 μA/cm^2 is located on electrode 13, while the nearest electrodes 12 and 14 also work as anodes but with lower current density.

The most common cathodic regions are electrodes 2 and 4 in the side channel and electrodes 5 and 15 in the main channel. The cathodic current density in these regions is equal or close to the corresponding anodic regions.

The other parts of the surface do not show stable behavior and change their state in different conditions. The central parts of the junction, namely, electrodes 9–11, work as cathodes and anodes in different conditions. Current densities on these electrodes do not exceed 12 μA/cm^2 for both current directions. The same behavior shows the electrodes located in the bottom part of the main channel, 6–8. In different flow conditions, they work as anodes or cathodes. The current density also does not exceed 12 μA/cm^2. Visual observation of the inner surface of the multielectrode unit showed that the electrodes that worked as anodes were covered with brown corrosion products. At the same time, the electrodes that worked as cathodes remained clean. Visual observation is in agreement with the current measurements.

The analyses of flow distribution (Figure 1) in T-shape junction and 3D map of current distribution (Figure 7) reveal several differential aeration pairs. The first differencial aeration pair is located right in the junction. Here, the flow rate velocity changes greatly in the cross section of the pipe, accelerating in the top part of the side channel and slowing in the bottom part, forming a stagnant zone. Thus, electrode 1 becomes an anode and the closest electrodes 2, 4, and 5 become cathodes. Depending on the flow rate, the anodic

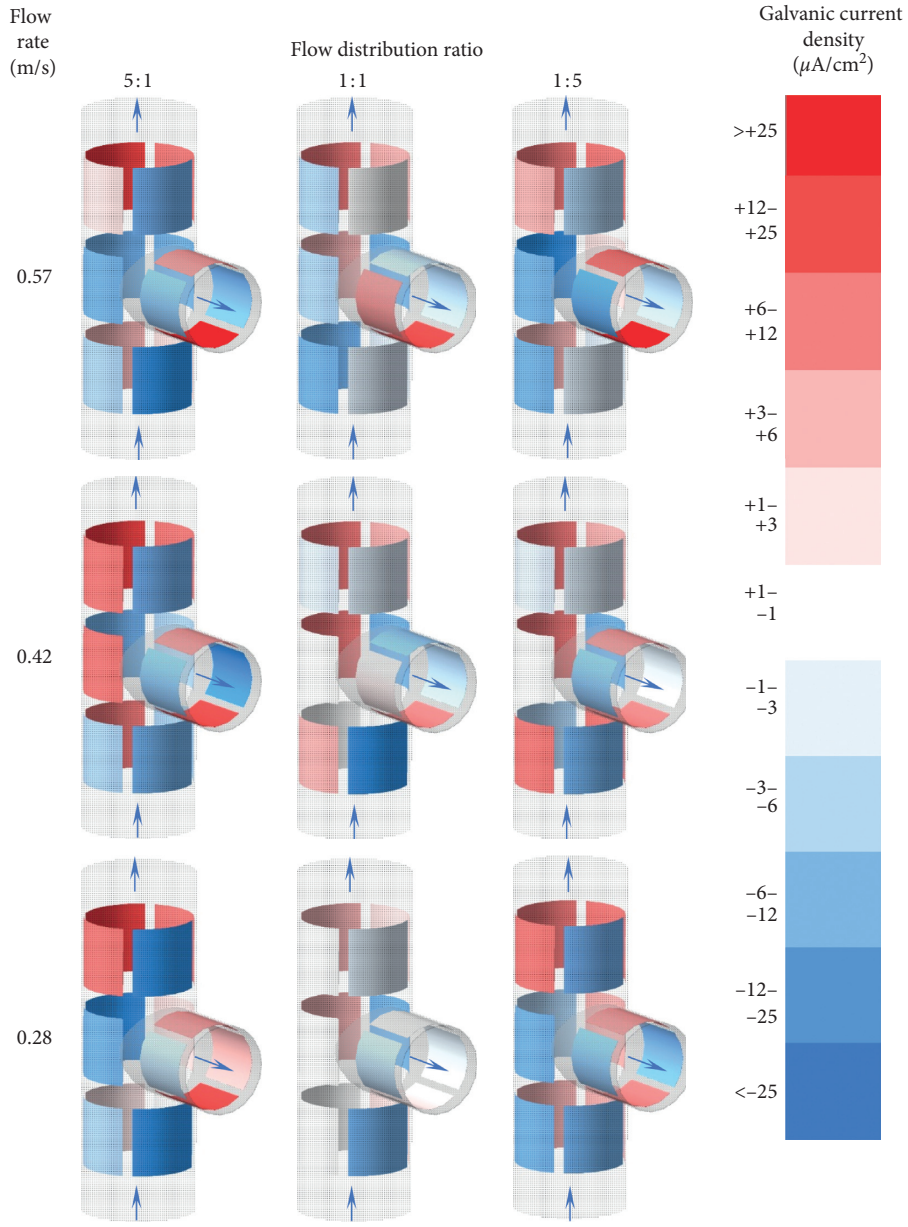

Figure 7: A 3D map of anodic and cathodic regions distribution in the T-shape junction depending on the flow rate and flow distribution ratio at 20°C in tap water.

current density on electrode 1 may reach 25 mA/cm^2, which causes accelerated corrosion in this region, up to 0.3 mm/year or even higher.

Another differential aeration cell is located in the main channel after the junction. Here, the flow rate also has dissimilar rate through the cross section of the pipe. Electrode 15 becomes the cathode, and electrode 13 is an anode. The electrodes between this pair most often are anodes; however, the current density on them is lower than that on electrode 13.

The analyses of differential aeration pair operation are important from a practical point of view. The operation regime of T-shape junction was found to allow minimizing local anodic current in the differential aeration cells. For the tap water, the lowest local anodic current was registered when flow rate did not exceed 0.42 m/s and water distribution ratio in the junction was 1 : 1 and higher. These results might be used for projecting water distribution systems to reduce potential galvanic corrosion. Furthermore, this reveals the most vulnerable corrosion places of the junction, where corrosion protection measures require more attention.

4. Conclusions

This paper investigates the distribution of local currents in the inner surface of the T-shape junction of steel pipes depending on the flow rate (0.28–0.52 m/s) and water distribution ratio (5 : 1 to 1 : 5). The formation of differential aeration cells was established, and their influence on the corrosion was discussed:

Flow distribution in T-shape junction leads to the formation of stagnant regions in the bottom part of the side channel and in the part opposite to the junction part of the main channel after the junction. The flow rate in this region is 3–5 times slower than that the inlet flow rate. The accelerated flow rate regions are formed in the top part of the main channel and in the top part of the side channel, where the flow rate can double the inlet rate.

The flow distribution leads to the formation of differential aeration cells. One anodic region is located in the bottom part of the side channel. The cathodic regions are located around it, in the side walls of the side channels and in the top part of the main channel before the junction. The anodic current density in this region may exceed $25\,\mu A/cm^2$, which equals 0.3 mm/year corrosion penetration rate. Another anodic region, less localized, is located in the bottom part of the main channel after the junction. The cathode is mainly located on the top side of the main channel. Here, anodic current density does not exceed $12\,\mu A/cm^2$.

The regime for the lowest galvanic current was established. For the tap water of 20°C temperature, the lowest local anodic current was measured when flow rate did not exceed 0.42 m/s and water distribution ratio between main and side channel in the junction was 1 : 1 and higher.

The obtained results agree well with the flow distribution in the junction and will be helpful for projection and maintenance of the pipe junctions to prevent localized corrosion and shortage of the operation time.

Data Availability

All data generated or analyzed during this study are included within the article.

Conflicts of Interest

The author declares that there are no conflicts of interest regarding the publication of this paper.

Acknowledgments

This work was supported by the Ministry of Education and Science of Ukraine (grant nos. 2044 and 2017).

References

[1] G. S. Vasyliev, "The influence of flow rate on corrosion of mild steel in hot tap water," *Corrosion Science*, vol. 98, pp. 33–39, 2015.

[2] H. S. Vasyl'ev and Y. S. Herasymenko, "Corrosion meters of new generation based on the improved method of polarization resistance," *Materials Science*, vol. 52, no. 5, pp. 1–10, 2017.

[3] G. Vasyliev, "Polarization resistance measurement in tap water: the influence of rust electrochemical activity," *Journal of Materials Engineering and Performance*, vol. 26, no. 8, p. 3939, 2017.

[4] R. Y. Herasymenko, H. S. Vasyl'ev, and Y. S. Herasymenko, "Elevation of the reliability of corrosion monitoring of low-carbon steel in tap water," *Materials Science*, vol. 53, no. 3, p. 337, 2017.

[5] G. S. Vasyliev, "Adaptation of the method of polarization resistance to the evaluation of corrosion rate in the formation of deposit of difficultly dissolved iron oxides," *Materials Science*, vol. 55, no. 1, pp. 130–135, 2019.

[6] Š. Msallamová, P. Novák, M. Kouřil, and J. Stoulil, "The differential aeration cell and the corrosion paradox," *Materials and Corrosion*, vol. 66, no. 5, pp. 498–503, 2015.

[7] J. De Gruyter, S. F. L. Mertens, and E. Temmerman, "Corrosion due to differential aeration reconsidered," *Journal of Electroanalytical Chemistry*, vol. 506, no. 1, pp. 61–63, 2001.

[8] Y.-C. Chang, R. Woollam, and M. E. Orazem, "Mathematical models for under-deposit corrosion," *Journal of The Electrochemical Society*, vol. 161, no. 6, pp. C321–C329, 2014.

[9] R. B. Petersen and R. E. Melchers, "Long-term corrosion of cast iron cement lined pipes," *Annual Conference of the Australasian Corrosion Association*, vol. 2012, pp. 146–157, 2012.

[10] R. E. Melchers and T. Wells, "Correlation between soil electrical resistivity, polarisation resistance and corrosion of steel," *Corrosion Engineering, Science and Technology*, vol. 53, no. 7, pp. 524–530, 2018.

[11] M. Miyasaka, K. Kishimoto, and S. Aoki, "Study on differential aeration cell corrosion owing to differential flow rate," *Zairyo-to-Kankyo*, vol. 40, no. 6, pp. 401–405, 1991.

[12] D.-L. Zhang, W. Wang, and Y. Li, "An electrode array study of electrochemical inhomogeneity of zinc in zinc/steel couple during galvanic corrosion," *Corrosion Science*, vol. 52, no. 4, pp. 1277–1284, 2010.

[13] H. Ju, J. Duan, Y. Yang, N. Cao, and Y. Li, "Mapping the galvanic corrosion of three coupled metal alloys using coupled multielectrode array: influence of chloride ion concentration," *Materials*, vol. 11, no. 4, p. 634, 2018.

[14] S. S. Jamali and D. J. Mills, "Studying inhomogeneity of organic coatings using wire beam multielectrode and physicomechanical testing," *Corrosion Engineering, Science and Technology*, vol. 48, no. 7, pp. 489–495, 2013.

[15] L. Yang and N. Sridhar, "Coupled multielectrode array systems and sensors for real-time corrosion monitoring—a review," in *Proceedings of the NACE—International Corrosion Conference Series*, pp. 66811–668145, San Diego, CA, USA, March 2006.

[16] L. Yang, K. T. Chiang, P. K. Shukla, and N. Shiratori, "Internal current effects on localized corrosion rate measurements using coupled multielectrode array sensors," *Corrosion*, vol. 66, no. 11, Article ID 115005, 2010.

[17] A. Naganuma, K. Fushimi, K. Azumi, H. Habazaki, and H. Konno, "Application of the multichannel electrode method to monitoring of corrosion of steel in an artificial crevice," *Corrosion Science*, vol. 52, no. 4, pp. 1179–1186, 2010.

[18] F. Varela, M. Y. J. Tan, and M. Forsyth, "An electrochemical method for measuring localized corrosion under cathodic protection," *ECS Electrochemistry Letters*, vol. 4, no. 1, pp. C1–C4, 2014.

[19] K. Wang, F. B. Varela, and M. Y. Tan, "An array of multi-electrodes for locating, visualizing, and quantifying stray current corrosion," *Corrosion*, vol. 74, no. 10, pp. 1093–1101, 2018.

[20] Y. Xu and M. Y. Tan, "Probing the initiation and propagation processes of flow accelerated corrosion and erosion corrosion under simulated turbulent flow conditions," *Corrosion Science*, vol. 151, pp. 163–174, 2019.